Splitting of electronic levels with positive and negative angular momenta in $In_{0.53}Ga_{0.47}As/InP$ quantum dots by a magnetic field

M. Bayer, O. Schilling, and A. Forchel
Technische Physik, Universität Würzburg, Am Hubland, D-97074 Würzburg, Germany

T. L. Reinecke
Naval Research Laboratory, Washington, D.C. 20375

P. A. Knipp
Department of Physics and Computer Science, Christopher Newport University, Newport News, Virginia 23606

Ph. Pagnod-Rossiaux and L. Goldstein
Alcatel-Alsthom Recherche, F-91460 Marcoussis, France

(Received 1 December 1995)

High excitation magnetoluminescence investigations have been performed on cylindrical $In_{0.53}Ga_{0.47}As/InP$ quantum dots with different diameters down to 30 nm. The magnetic field oriented normal to the quantum disks enhances the lateral confinement of the carriers inside of the dots, and splits energy levels with positive and negative angular momenta due to the Zeeman-like interaction. This splitting depends linearly on B, and is independent of the disk size. The increase of the lateral quantization of the carriers by the magnetic field, on the other hand, depends strongly on the dot diameter. The experimental results are in good agreement with the results of detailed numerical calculations. [S0163-1829(96)00223-8]

Due to the potential advantages of quasi-zero-dimensional semiconductor structures for technological applications,[1–3] great efforts have been made to fabricate high-quality quantum dots. These nanostructures represent artificially created atomiclike systems with electronic properties which can be controlled by fabrication. The technological efforts can be mainly divided into two categories: One is the direct epitaxial growth of the structures,[4] the other the lithographical patterning of epitaxial layers.[5]

Experiments in high magnetic fields are a particularly powerful tool for the investigation of such dot systems. The energy levels of quantum dots are fully quantized, and are characterized by three spatial quantum numbers and the spin quantum number. The magnetic field B defines a preferential direction in space and therefore lifts degeneracies due to geometrical symmetries, as is known from atomic physics. In addition, B enhances the confinement of the carriers in the dots. Magnetic-field experiments are therefore expected to give a direct insight into the energy-level structure of quantum dots. Despite a large number of theoretical investigations,[6–15] only a few magneto-optical studies on quantum-dot arrays have been reported up to now, both in far-infrared and photoluminescence experiments.[16–20] These studies have focused on GaAs-based quantum dots of a single average size. Here we have investigated InP-based quantum dots of different diameters. The $In_{0.53}Ga_{0.47}As/InP$ material system has a low surface recombination velocity. Therefore it permits the fabrication of etched quantum-wire and -dot structures with dimensions down to the 10-nm range.[21]

We have performed detailed luminescence studies of $In_{0.53}Ga_{0.47}As/InP$ quantum dots in magnetic fields up to 10.5 T. The magnetic field was aligned parallel to the symmetry axis of the cylindrical dots. High optical excitation enabled us to observe emission from dot levels of different magnetic quantum numbers n_φ corresponding to different angular momenta. Levels of the same absolute value $|n_\varphi|=1$, which are degenerate at $B=0$, are split by the interaction of their magnetic moment with the magnetic field. This splitting is expected to depend only on the angular momentum and to be independent of the dot size and linear in B. We compare our experimental findings with the results of detailed numerical calculations that include the full geometric confinement potentials.

The quantum dots were fabricated by high-resolution electron-beam lithography and wet chemical etching on a 5-nm-wide $In_{0.53}Ga_{0.47}As$ quantum well sandwiched between two InP layers. Details of the fabrication process have been given earlier.[21] For the quantum-well parameters only one electron subband is confined in the quantum well. In addition, the heavy-hole–light-hole splitting is about 70 meV, which is larger than the region of interest for all lateral quantization effects in our experiments. Therefore heavy-hole character can be attributed to the topmost valence-band states. Figure 1 shows a scanning electron micrograph of a dot pattern containing dots of a single size. From this micrograph the dot diameter can be estimated to be 38 nm with an accuracy of ± 3 nm. The dots are to a good approximation cylindrical in shape, and were fabricated in 50×50-μm^2 arrays. Within an array the average dot size was kept constant. The dot diameters were varied between about 30 and 50 nm.

The samples were immersed in liquid helium ($T=1.8$ K) in an optical split coil magnetocryostat ($B<10.5$ T). A cw Ar^+ laser ($\lambda=514.5$ nm) was used for optical excitation with power densities of up to 5 kW cm^{-2}. The laser spot was focused to a diameter of about 75 μm, slightly larger than

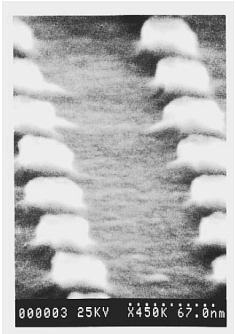

FIG. 1. Scanning electron micrograph of a pattern of cylindrical $In_{0.53}Ga_{0.47}As/InP$ quantum dots with an average diameter of (38 ± 3) nm.

the size of the dot patterns, in order to obtain a homogeneous excitation density. The emitted light was dispersed by a 0.32-m single-grating monochromator, and detected by a liquid-nitrogen-cooled Ge detector.

Figure 2 displays a series of high excitation spectra (power density 2.5 kW cm^{-2}) of 38-nm-diameter dots at different magnetic fields. At zero field a main line at 0.93 eV and a pronounced shoulder at 0.95 eV can be seen. The main line shifts continuously to higher energies with increasing magnetic field. Simultaneously the shoulder first broadens at low magnetic fields and then is seen to split at $B\geqslant4$ T. As indicated by the arrows in Fig. 2, the lower line which arises from this splitting shifts steadily to smaller energies, while the upper line moves to higher energies. The splitting between these two lines increases from about 10 meV at 5 T to more than 20 meV at 10 T.

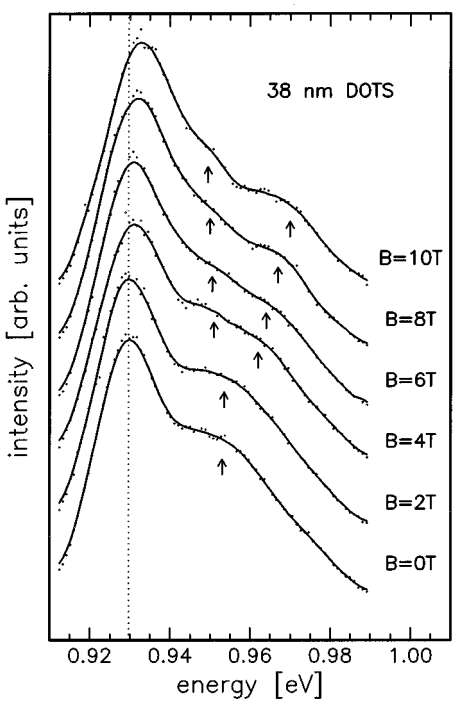

FIG. 2. High excitation spectra of 38-nm dots at different magnetic fields. The excitation power density was 2.5 kW cm^{-2}. For clarity the spectra are shifted vertically with respect to each other. The arrows indicate the splitting of the first excited transition. The dotted line indicates the position in energy of the ground-state transition at $B=0$.

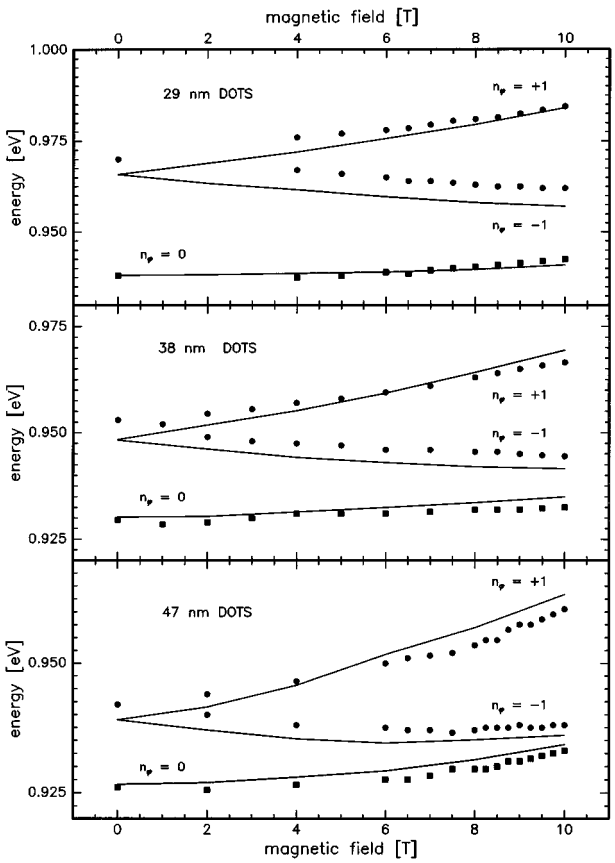

FIG. 3. Positions in energy of the interlevel transitions observed on 29-, 38-, and 47-nm dots as functions of the magnetic field. The symbols give the experimental data, the lines the results of the calculations.

The energies of the observed electron-hole transitions for the 38-nm dots are displayed in Fig. 3(b) for different magnetic fields. In Figs. 3(a) and 3(c) data obtained for 29- and 47-nm dots are shown. For all structures the ground state and the first excited transitions are observed at all values of B, including $B=0$. The splitting between these transitions increases with decreasing dot diameter due to the enhanced lateral quantization. In all cases the first excited transition is found to be split by the magnetic field, and the splitting increases continuously with increasing B.

We have performed detailed numerical calculations to understand the single-particle electron and hole states in these structures in nonzero magnetic field. Exciton effects are not expected at the high optical excitation used in the experiments, and they are therefore not included in the calculations. The full geometric confining potentials are taken into account.[22] Schrödinger's equation is in general not separable in this geometry. It therefore was discretized and solved by using the matrix diagonalization technique described in Ref. 23. The fully quantized levels of the cylindrical dots are characterized by three spatial quantum numbers n_z, n_r, and n_φ corresponding to motions in vertical, radial, and azimuthal directions.[24,25] The quantum number n_φ corresponds to the orbital angular momentum around the symmetry axis of the dots, and is equivalent to the magnetic quantum num-

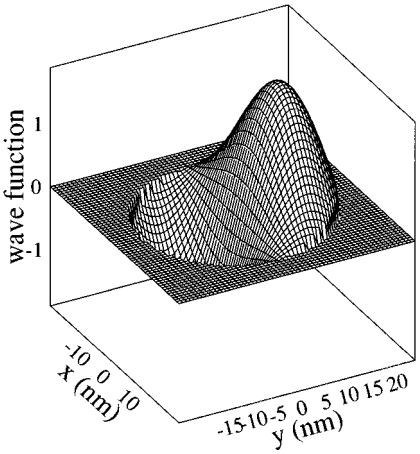

FIG. 4. Real part of the in-plane wave function of the electron state described by the radial quantum number $n_r=0$, and by the azimuthal quantum number $n_\varphi=\pm1$ at $B=0$.

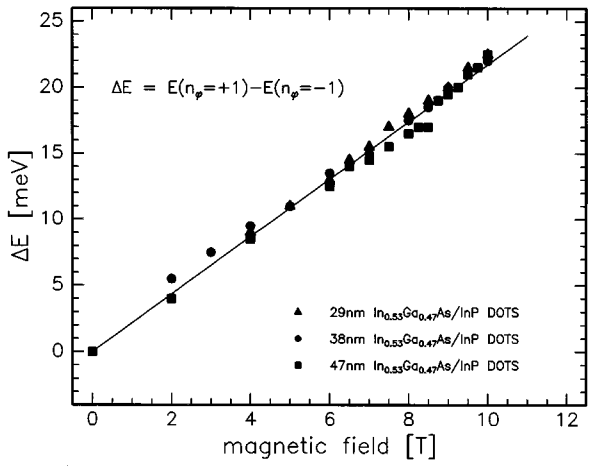

FIG. 5. Energy splitting between the transitions involving states of angular momenta $+1$ and -1. The data for three different dot diameters—29, 38, and 47 nm—are shown.

ber in atomic physics. The two lowest dot states at $B=0$ are described by the ground-state values of the vertical and radial quantum numbers for structures with diameters below 50 nm. The ground state has an angular momentum $n_\varphi=0$. The first excited states have angular momenta -1 and $+1$, and are degenerate at $B=0$.

The wave function of the carriers in the quantum dot plane—in a separable approximation—can be written as the product of angular momentum eigenstates and of the radial wave function $R(r)$,

$$\psi(r,\varphi)=\frac{1}{\sqrt{2\pi}}\,e^{in_\varphi\varphi}r^{|n_\varphi|}R(r). \tag{1}$$

In Fig. 4 we show the real part of the wave function $\mathrm{Re}(\psi)$ associated with angular momentum $n_\varphi=1$. States with equal positive and negative angular momenta have the same real parts. The s-like ground state $\mathrm{Re}(\psi)$ has no angular dependence. The real part of the p-like states with $n_\varphi=\pm1$ shows a modulation in φ in the plane of the quantum disks, as shown in Fig. 1. The absolute value of the angular momentum corresponds to the number of nodal planes normal to the disk. With increasing angular momentum, the carriers are pushed out of the center of the dot in radial direction because of the centrifugal potential $-n_\varphi^2 r^{-2}$ in Schrödinger's equation.

For an axially symmetric Hamiltonian the energies corresponding to motion in the plane can be written as a sum of an energy which describes the lateral geometric and magnetic confinement, and which we will call the confinement energy E_l in the following, plus a Zeeman-like interaction energy of the form

$$E=\tfrac{1}{2}\hbar\omega_c n_\varphi, \tag{2}$$

where $\hbar\omega_c=\hbar(eB)/m$ is the cyclotron energy of the carrier. The confinement energy expresses at $B=0$ the influence of the lateral geometric confinement potential, which is enhanced by the magnetic potential for nonzero B. This confinement energy depends only on the magnitude of n_φ and not on its sign. At low magnetic fields the cyclotron radius $\lambda_c=\hbar^{0.5}/(eB)^{0.5}$ is much larger than the dot diameters. Under this condition the dot diameter is the determining length in this quantization energy. With increasing magnetic field the cyclotron radius becomes comparable to the dot diameter, and then the magnetic contribution to the total confinement of the carriers becomes more and more important. At very high fields, finally, the magnetic length becomes less than the dot diameter, and the magnetic-field energy determines the quantization energy E_l.

The regimes of low ($\hbar\omega_c \ll E_l$) and high magnetic fields ($\hbar\omega_c \gg E_l$), in which either the geometric or magnetic quantization energy dominates E_l, are therefore defined by the relation between the cyclotron energy and the lateral geometric quantization energy. The cyclotron energy can be tuned by the magnetic field from zero up to about 22 meV for the highest fields available in the present experiments. The transition between the regimes takes place when the two energies become comparable. Consequently the confinement energy changes from a weak B^2-dependent shift at low fields to a strong, linear dependence on B at high fields. In the latter case the geometric confinement energy is relatively small, and the states are effectively transformed into Landau levels.

The Zeeman-like term expresses the interaction of the magnetic moment associated with the angular momentum of the carriers with the magnetic field, and lifts the degeneracy of levels with the same absolute value of angular momentum at nonzero fields. This Zeeman-like shift depends linearly on the magnetic field and is independent of the dot diameter, in contrast to the confinement energy.

The results of our calculations for the electron-hole transition energies of the dots of 29-, 38-, and 47-nm diameter are also shown in Fig. 3 as solid lines. Good overall agreement with the data is seen there. From Eq. (2) the splitting ΔE between the transitions arising from states with angular momenta $+1$ and -1 is given by

$$\Delta E_B=E(n_\varphi=+1)-E(n_\varphi=-1)=\Delta E_e+\Delta E_h, \tag{3}$$

$$\Delta E_B=\hbar\omega_c=\hbar\,\frac{eB}{\mu}, \tag{4}$$

where μ is the reduced effective mass of electrons and holes. As discussed above, the splitting is therefore expected to

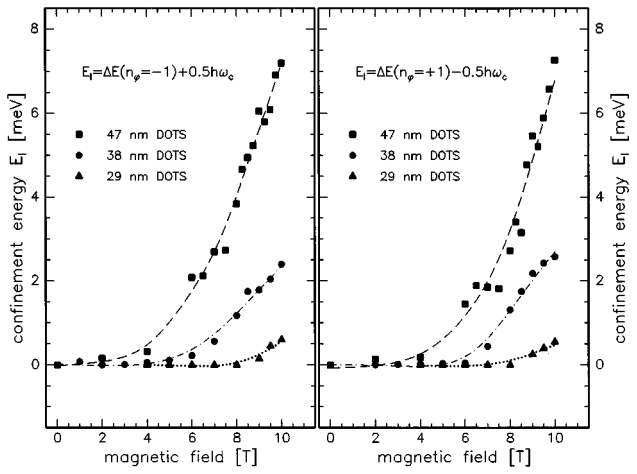

FIG. 6. Increase of the confinement energy by the magnetic field determined from the -1 (a) and $+1$ (b) transitions by subtracting the Zeeman-like energy. The data for the quantum dots with average diameters of 29, 38, and 47 nm are shown. The lines are guides to the eye.

increase linearly with magnetic field. It is also expected to be independent of the dot diameter. The experimentally measured difference in energy ΔE_B is shown in Fig. 5 for the three patterns with dot diameters of 29, 38, and 47 nm. Both the linear dependence of the energy splitting on B as well as the independence of ΔE_B on the dot size are confirmed by our experiments. From the experimentally determined ΔE_B, we extract a reduced mass of 0.051, which is within the experimental error, in good agreement with the reduced mass determined from the Landau-level splitting of a quasi-two-dimensional reference sample under similar high excitation conditions.

From Fig. 3 it is also seen that the splitting between the ground-state transition and the first excited transition ΔE_C at $B=0$ increases strongly with decreasing dot diameter. This splitting arises from the lateral quantization energy E_l, and is independent of the sign of the angular momentum. It is enhanced by the magnetic confinement potential. As already described, the relative contributions of the geometric and magnetic confinement energies depend on the relative size of the cyclotron energy and the geometric confinement energy. If one takes ΔE_C as a measure of the geometrical quantization energy, a comparison with the available cyclotron energies shows that the electronic properties of the largest, 47-nm-wide dots can be investigated both in the low- and high-field regimes. As can be shown, all states with $n_r=0$ and with negative values of the angular momentum n_φ converge at high fields, with the ground state $n_\varphi=0$ in the lowest Landau level.

In contrast, for the smaller structures the high-field limit cannot be reached in the present experiments at $B<10.5$ T: For the 38-nm dots an intermediate-field regime can be obtained, in which the changeover from geometric to magnetic quantization occurs, whereas the 29-nm dots always show low-field behavior, since ΔE_B is always smaller than ΔE_C. This can be also seen from the almost linear dependence of the -1 and $+1$ transition energies on the magnetic field. Furthermore the almost symmetric splitting of the $n_\varphi=\pm 1$ states relative to the observed transition energy at $B=0$ shows that the magnetic field affects the energies of the carriers only via the Zeeman-like energy.

Because the influence of the Zeeman-like energy is well known, the confinement energy can be obtained from the observed transition energies by subtracting the Zeeman-like energy for the dots of different diameters. In this way we obtain the confinement energy E_l as a function of the magnetic field. The results for 29-, 38-, and 47-nm-wide dots are shown in Figs. 6(a) and 6(b). The data were determined both for the -1 transition [Fig. 4(a)] and for the $+1$ transition [Fig. 4(b)]. For the smallest, 29-nm-wide dots only a weak increase of the localization energy by the magnetic field is seen at magnetic field above 8 T. The data taken from the largest dots, in contrast, show, above 5 T, a strong linear dependence on B, indicating the high-field regime. At low magnetic fields E_l is only slightly increased, and the data are consistent with a B^2 dependence. A relatively weak field dependence is observed for the dots of 38-nm diameter up to $B\leqslant 7$ T. At higher fields there are indications of a beginning transition to the high-field regime.

In order to characterize the dependence of the transformation between low- and high-field behaviors on the dot diam-

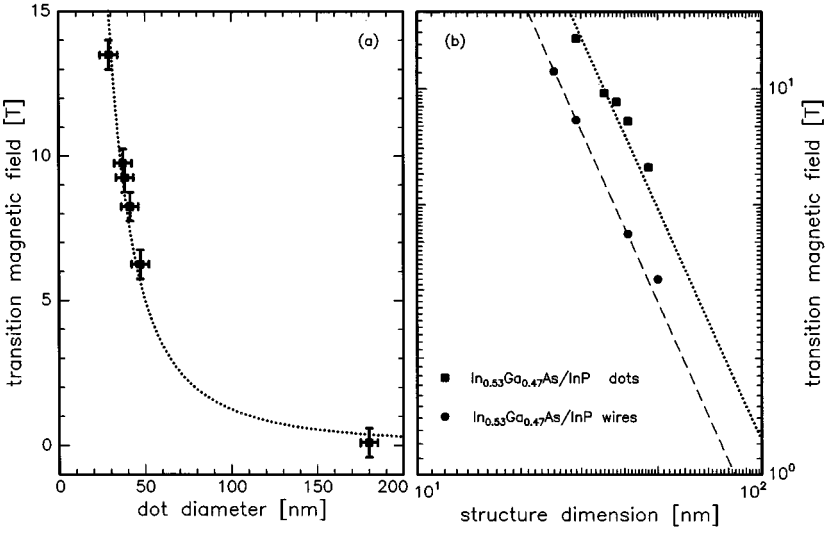

FIG. 7. (a) Transition magnetic field defined in the text as a function of the dot diameter. (b) Comparison of the transition magnetic fields for $In_{0.53}Ga_{0.47}As/InP$ quantum wires and quantum dots.

eter, we have defined a transition magnetic field B_T. B_T is the magnetic field at which the transition from predominant geometric to predominant magnetic quantizations occurs. B_T is defined as the field strength B_T at which the localization energy E_l is increased by 2 meV. This definition is similar to that used by us earlier for $In_{0.53}Ga_{0.47}As/InP$ quantum wires.[26] For the smallest dots we determine a value for B_T by extrapolating the low-field data.

The results for B_T are shown in Fig. 7(a) as a function of the dot diameter. B_T increases strongly with decreasing dot diameter, which can be understood in the following way: Since the transition takes place when the magnetic quantization potential exceeds the geometric one, B_T should depend inversely on the square of the dot radius:

$$\hbar\omega_c = \hbar \frac{eB_T}{m} \approx \Delta E_c \sim \frac{1}{r^2}. \tag{5}$$

As shown by Fig. 7(a), the experimentally determined values for B_T can be described well by such a functional dependence. In Fig. 7(b) the transition magnetic fields B_T for $In_{0.53}Ga_{0.47}As/InP$ quantum wires and quantum dots are compared for structures of different lateral widths. Similar to the dots, the wires show the proportionality of B_T to the inverse square of their lateral sizes. The values of B_T for dots are significantly higher than those for wires, due to the confinement in an additional direction, i.e., to the reduced dimensionality of dots in comparison to wires.

In conclusion, we have studied the splitting between $In_{0.53}Ga_{0.47}As/InP$ quantum-dot states of angular momenta $+1$ and -1 by the magnetic field in luminescence experiments, and have compared our results with detailed numerical calculations. We observe a linear dependence of the splitting on the magnetic field. Studies of dots with varying sizes show that the Zeeman-like splitting is independent of the dot size. The characteristic field for the transition from predominantly geometrically to predominantly magnetically confined states is found to be inversely proportional to the diameter of the dots.

We gratefully acknowledge the financial support of this work by the Deutsche Forschungsgemeinschaft, the ESPRIT Basic Research Program, the U.S. Office of Naval Research, and the Office of International Studies of Christopher Newport University.

[1] Y. Arakawa and H. Sakaki, Appl. Phys. Lett. **40**, 939 (1982).
[2] Y. Arakawa, K. Vahala, and A. Yariv, Appl. Phys. Lett. **45**, 950 (1984).
[3] M. Asada, Y. Myamoto, and Y. Suematsu, Jpn. J. Appl. Phys. **24**, L95 (1988).
[4] See, for example, R. Nötzel, N. N. Ledentsov, L. Däweritz, M. Hohenstein, and K. Ploog, Phys. Rev. Lett. **67**, 3812 (1991); D. Leonard, M. Krishnamurty, C. M. Reaves, S. P. DenBaars, P. M. Petroff, Appl. Phys. Lett. **63**, 3203 (1993); J. M. Moison, F. Houzay, F. Barthe, L. Leprince, E. Andre, and O. Vatel, *ibid*. **64**, 196 (1994); M. Sopanen, H. Lipsanen, and J. Ahopelto, *ibid*. **66**, 2364 (1995), N. N. Ledentsov *et al.*, in *Proceedings of the 22nd International Conference on the Physics of Semiconductors*, edited by D. J. Lockwood (World Scientific, Singapore, 1995), p. 1855.
[5] See, for example, K. Kash, A. Scherer, J. M. Worlock, H. G. Craighead, and M. C. Tamargo, Appl. Phys. Lett. **49**, 1043 (1986); J. Cibert, P. M. Petroff, G. J. Dolan, S. J. Pearton, A. C. Gossard, and J. H. English, *ibid*. **49**, 1275 (1986); M. Notomi, M. Naganuma, T. Nishida, T. Tamamura, H. Iwamura, S. Nojima, and M. Okamoto, *ibid*. **58**, 720 (1991); P. Ils, M. Michel, A. Forchel, I. Gyuro, M. Klenk, and E. Zielinski, *ibid*. **64**, 496 (1994).
[6] V. Fock, Z. Phys. **47**, 446 (1928).
[7] P. A. Maksym and T. Chakraborty, Phys. Rev. Lett. **65**, 108 (1990).
[8] F. M. Peeters, Phys. Rev. B **42**, 1486 (1990).
[9] F. Geerinckx, F. M. Peeters, and J. T. Devreese, J. Appl. Phys. **68**, 3435 (1990).
[10] T. Chakraborty, V. Halonen, and P. Pietiläinen, Phys. Rev. B **43**, 14 289 (1991).
[11] A. O. Govorov and A. V. Chaplik, Zh. Eksp. Teor. Fiz. **99**, 1853 (1991) [Sov. Phys. JETP **72**, 1037 (1991)].
[12] D. Pfannkuche and R. R. Gerhardts, Phys. Rev. B **44**, 13 132 (1991).
[13] V. Halonen, T. Chakraborty, and P. Pietiläinen, Phys. Rev. B **45**, 5980 (1992).
[14] P. Hawrylak and D. Pfannkuche, Phys. Rev. Lett. **70**, 485 (1993).
[15] S. Nomura, Y. Segawa, and T. Kobayashi, Phys. Rev. B **49**, 13 571 (1994).
[16] Ch. Sikorski and U. Merkt, Phys. Rev. Lett. **62**, 2164 (1989).
[17] T. Demel, D. Heitmann, P. Grambow, and K. Ploog, Phys. Rev. Lett. **64**, 788 (1990).
[18] Y. Nagamune, M. Nishioka, S. Tsukamoto, and Y. Arakawa, Appl. Phys. Lett. **64**, 2495 (1994).
[19] A. Zrenner, L. V. Butov, M. Hagn, G. Abstreiter, G. Böhm, and G. Weimann, Phys. Rev. Lett. **72**, 3382 (1994).
[20] M. Bayer, A. Schmidt, A. Forchel, F. Faller, T. L. Reinecke, P. A. Knipp, A. A. Dremin, and V. D. Kulakovskii, Phys. Rev. Lett. **74**, 3439 (1995).
[21] P. Ils, A. Forchel, K. H. Wang, P. Pagnod-Rossiaux, and L. Goldstein, Phys. Rev. B **50**, 11 746 (1994).
[22] The single-particle energies have already been calculated in Ref. 6 for a quantum dot with a parabolic lateral confinement potential. For the present dot structures the lateral confinement is of rectangular shape, and therefore the results of V. Fock cannot be used in order to describe the experimental data satisfactorily.
[23] Ch. Gréus, R. Spiegel, F. Faller, A. Forchel, P. A. Knipp, and T. L. Reinecke, Phys. Rev. B **49**, 5753 (1994); M. Bayer, A. Forchel, I. E. Itskevich, T. L. Reinecke, P. A. Knipp, Ch. Gréus, R. Spiegel, and F. Faller, *ibid*. **49**, 14 782 (1994).
[24] R. H. Dicke and J. P. Wittke, *Introduction to Quantum Mechanics* (Addison-Wesley, Reading, MA, 1960), Chap. 15.
[25] The spin is neglected in our considerations since its contribution to the single-particle energies is negligible in comparison to the other contributions by the geometric and magnetic confinement potentials.
[26] M. Bayer, P. Ils, M. Michel, A. Forchel, T. L. Reinecke, and P. A. Knipp, Phys. Rev. B **53**, 4668 (1996).